

An experimental investigation on the normal force behavior of magnetorheological suspensions

ChaoYang Guo¹, XingLong Gong^{1*}, ShouHu Xuan¹, YanLi Zhang² and WanQuan Jiang²

¹CAS Key Laboratory of Mechanical Behavior and Design of Materials, Department of Modern Mechanics, University of Science and Technology of China, Hefei, 230027, China

²Department of Chemistry, University of Science and Technology of China, Hefei, 230026, China

(Received November 10, 2011; final revision received April 23, 2012; accepted April 30, 2012)

Abstract

In this work the normal force behavior of magnetorheological suspensions are systematically investigated. Four magnetorheological suspensions with different volume fractions (10%, 20%, 30%, and 40%) are prepared and both the static and dynamic normal forces of the samples are measured by using a commercial plate-plate magneto-rheometer under constant and sweeping magnetic field. A positive normal force will be generated when the applied magnetic field exceeds a critical value. The normal force firstly increases with the increasing of magnetic field strength and then reaches a saturation value. A magnetization model is utilized to represent this mechanism. The oscillatory dynamic normal forces with time are studied and their changes with shear rates are dependent on the volume fraction. Comparisons between static and dynamic normal forces show that the differences between them are dependent on the volume fraction and magnetic field. The temperature effect on the normal force is studied and under high magnetic field the normal force would increase slightly with the increasing of temperature.

Keywords: normal force, magnetorheological suspension, magnetorheological fluid, temperature

1. Introduction

Magnetorheological suspension (MRS) or magnetorheological fluid (MRF), invented by Rabinow in the 1940s, is a smart material consisting of magnetic particles dispersed in non-magnetic liquid such as oil or water. This material exhibits fast, strong and reversible changes in its rheological property when a magnetic field is applied, making it very interesting for lots of applications (Carlson *et al.*, 1996; Kordonsik *et al.*, 2000; Spencer Jr *et al.*, 2003; Li *et al.*, 2007; Hiemenz *et al.*, 2008; Chen and Liao, 2008; Wang *et al.*, 2009). The rheological properties or force behaviors of MR suspensions can be divided into two aspects: shear response in the direction perpendicular to that of magnetic field and normal behavior along the field direction. Most of the studies on the MRS have focused on the perpendicular field dependent shear response (Ginder *et al.*, 1994; Yong *et al.*, 2009) and the researches on the normal force behavior are relatively rare.

Normal forces of magnetorheological fluids are very important for designing precision MR devices and MRF polishing, evaluating the rheological properties of the material, and understanding the structure deformation of the magnetorheological fluids. Shkel and Klingenberg (2000)

made the theoretical calculation showing that the normal stress σ_{33} and the magnetic field intensity H can be expressed as $\sigma_{33} \propto H^2$. In 2002, Vicente *et al.* (2000) firstly experimentally studied the normal force of the concentrated MR suspension, which containing 50% volume fraction carbonyl iron particles, by using a commercial controlled stress parallel-plate rheometer. They found the normal force could be generated when two criteria were satisfied: the magnetic field must reach a critical value and the MRS must be under shearing. The positive and strain dependent normal force reached a maximum with the increasing of the shearing strain. However, See and Tanner (2003) found that the normal force generated and acted to push the plates apart even when the MRS was not subject to any deformation. It increased with the increasing of the magnetic flux density. Moreover, the normal force decreased with increasing of the shear strain, and eventually reached a plateau value. Then Laun *et al.* (2008) investigated the first and second normal stress differences of a 50% volume fraction MR fluid by using a commercial magneto-rheometer with plate-plate and cone-plate geometry. Without shear, the static normal force F_N for plate-plate increased with magnetic flux density as a power law: $F_N \propto B^{2.4}$. The first normal stress difference N_1 was positive and about five times larger than the shear stress. The second normal stress difference N_2 was also positive. Chan *et al.* (2009; 2011)

*Corresponding author: gongxl@ustc.edu.cn

described an experimental study on the characteristics of an excited MR fluid in the field direction using a self-developed two-plate rheometer. The normal force of an MRF was increased with increasing of the B-fields and the relation was also confirmed with a power law having an exponent of about 2. The normal force can be further increased by imposing shear actions on the excited MRF. They used a mathematical model on the basis of the particle chain tilt phenomenon to describe this. Recently, López-López *et al.* (2010) reported a theoretical model based on the equilibrium between hydrodynamic and magnetostatic torques and forces in a field-induced aggregate of particles subjected to shear, especially they took into account the inhomogeneity of the applied field and explained the disagreement between the work by Vicente *et al.* (2002) and these by Laun *et al.* (2008) and See and Tanner (2003). Jiang *et al.* (2011) studied experimentally the dependence of the normal stress on the shear rate and magnetic field strength in the shear flow of magnetorheological (MR) fluids. Especially they showed that the normal stress increased considerably decreased suddenly and significantly upon the onset of shear thickening in MR fluids. The ratio of shear stress to normal stress was discussed and it increased with increase of the shear rate, but decreased with increase of the applied magnetic field. However, to the best of our knowledge, it has not been systemically investigated how the static and dynamic normal forces depend on the iron concentration, the type of externally applied magnetic field, temperature and any other parameters.

In this work, a series of magnetorheological suspensions with different iron concentrations were prepared and their normal forces were systemically tested and discussed. At first, by using a commercial plate-plate magneto-rheometer, the static and dynamic normal forces for the various concentration MR suspensions were measured under stationary or shearing condition. Both constant magnetic field and sweeping magnetic field have been employed to investigate their influence on the normal forces. Then a magnetization model is utilized to represent the variation of normal forces with magnetic field. The influences of shear rates on dynamic normal forces are observed. Comparisons between dynamic and static normal force were made. At last, the temperature effect on the normal force was studied. It will give us a comprehensive understanding of normal forces of MR fluids.

2. Experimental

2.1. Materials

MR suspensions were composed of carbonyl iron powder particles in silicone oil. The carbonyl iron particles were purchased from BASF (model CN) whose average particle size was about 6 μm . Silicone oil (H201) was purchased from Sinopharm Chemical Reagent Co. Ltd and the

viscosity of silicone oil was about 20 mPa·s. A small amount of stearic acid (2 wt%) was added to prevent sedimentation occurring and ensure easy redispersibility after long term rest, due to the large density mismatch of the particles and the base oil (Zhang *et al.*, 2008; Jiang *et al.*, 2011). Four different MRS samples with iron particle volume fractions of 10%, 20%, 30% and 40% were prepared. The samples were vigorously shaken to ensure the required homogeneity before measurements.

2.2. Apparatus

The normal forces of MR suspensions were measured using a plate-plate magneto-rheometer (Physica MCR301, Anton Paar, Austria) with a temperature controller. The diameter of the plate was 20 mm and the plate gap was fixed at 1 mm. The magnetic field was applied normally to the sample plate via the magnetorheological unit (Physica MRD 180) and the temperature controller made sure that the tests could be taken at different temperatures from 0 to 100°C by using a water bath. The normal force was measured with a sensor built into air bearing and it could be recorded from -50 to 50 N with an accuracy of 0.03 N.

2.3. Methods

Two types of experiments were performed to study the static and dynamic normal forces. In all cases, the samples were sheared in a shear flow beforehand. The samples were sheared without a magnetic field at 50/s for 150 seconds to ensure good dispersion. Then, the shearing was then stopped for 30 seconds to equilibrate the sample. At last, the normal force was measured with different methods as follow.

Magneto-constant experiments: The constant magnetic field was applied and the normal force was monitored with time: static normal force was got without shearing while dynamic normal force was obtained under steady shear rate. This method is used to understand how the normal forces vary with time.

Magneto-sweep experiments: For static normal force, the samples were then excited by linear-sweeping magnetic field from 0 to 227 kA/m without shearing; for the dynamic normal force, the samples were then excited in the same way under steady shear rate. These testing can directly show the relation between the normal forces and magnetic field.

All the tests were repeated for three times to guarantee the validity of the results and the temperature was fixed at 25°C except for studying the temperature effect on normal forces.

3. Results and Discussion

3.1. Static normal force

Static normal forces which were measured by the magneto-constant method were firstly obtained when the magnetic field was kept as a constant value and no torsional

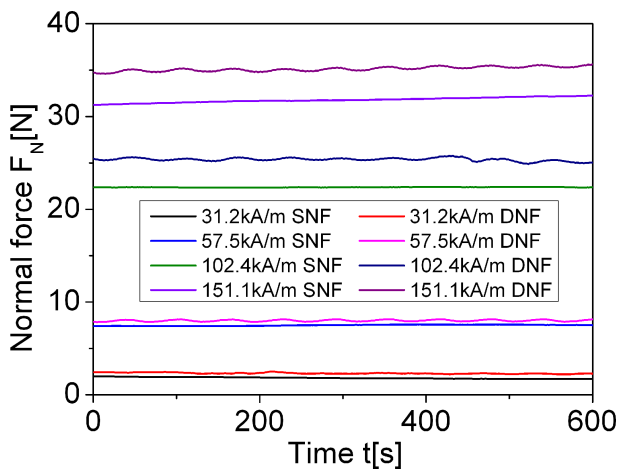


Fig. 1. (Color online) Static normal forces (SNF) and dynamic normal forces (DNF, shear rate is 1/s) during 600 s under various magnetic fields for 30% MR suspension.

motion was applied. For 30% MR suspension (Fig. 1), under low magnetic field strength the static normal forces decrease with the increasing of the testing time and tend to a steady value F_N . Besides, under low magnetic field (e.g. 31.17 kA/m), the time needed is longer than that under high magnetic field (e.g. 102.4 kA/m). The value of normal forces fluctuate slightly under low magnetic field, however, they keep steady during all the testing time at high magnetic field. Within a high magnetic field, the magnetic attractive force is bigger than the one in the small magnetic field and drives the particles align along the flux and form a chain structure more quickly and steady. Under a higher magnetic field 151.1 kA/m the static field normal forces increase a little with increasing of the testing time. However, the static normal force changes obscurely and can be regarded as a constant value. A similar phenomenon can also be found for other MR suspensions (not shown here for brevity). Thus, a 10 min period was adopted as the standard waiting time for testing the static normal force.

The steady static normal forces F_N for the four MR suspensions are extracted and plotted as a function of magnetic field strength, as shown in Fig. 2(a). As soon as the magnetic field is applied, the normal force generates and shows a positive value, meaning the sample is tending to push apart the two plates. With increasing of the externally applied magnetic field the normal force increases. A similar phenomenon can be obtained where static normal forces are measured by using the magneto-sweep method. As shown in Fig. 2(b), the applied magnetic field strength increases linearly from 0 to 227 kA/m and the highest magnetic field is larger than that in magneto-constant method. The magneto-sweep method can help us understand normal forces of as-prepared MRS more easily and directly than magneto-constant method. In comparison to the value obtained by magneto-constant method, the one

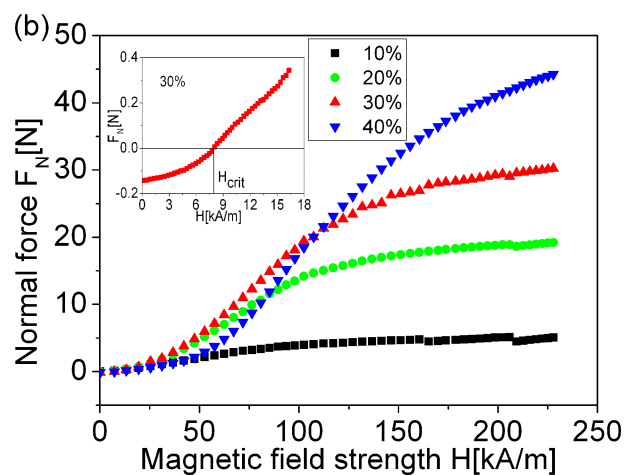
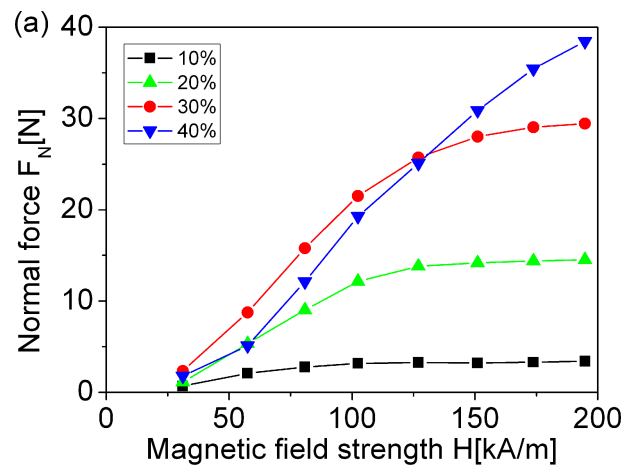


Fig. 2. (Color online) Static normal force with magnetic field strength measured by (a) magneto-constant method and (b) magneto-sweep method (the insert of (b) shows the normal forces of 30% MRF under small magnetic field).

tested by the magneto-sweep method is higher, which is because less testing time is used for the magneto-sweep method (as the static normal force decreases with time).

Notably, the normal force F_N increases with the increasing of the magnetic field strength H , and reaches a plateau value finally. This result indicates that the normal forces of the MRS can be saturated under a certain externally applied magnetic field, which is very similar to the shear yield stress saturation of MR suspensions (Ginder *et al.*, 1994; Jolly *et al.*, 1996; Shkel and Klingenberg, 2000; Fang *et al.*, 2009). For low fraction samples, such as 10% and 20% MRS, the saturation values are about 3 and 14 N when the applied magnetic field strength is 100kA/m. However, for 40% MRS, the normal force doesn't reach the saturation value even under a 227 kA/m magnetic field strength. In this case, larger magnetic field strength is needed for higher volume fraction sample to make all the magnetic particles be saturated. Therefore, the higher volume fraction sample often leads to a higher saturation mag-

netic field. To our knowledge, no similar observation has been reported. In the previous work, the volume fraction of the samples was higher and the applied magnetic field was smaller than these in our study. Therefore, the saturation phenomenon can not be found.

In addition, at a high magnetic field, the static normal forces increase when the volume fraction of the sample increases from 10% to 40%. Under the low magnetic field (<125 kA/m) the static normal forces increase when the volume fraction increases from 10% to 30%. However, they decrease when the volume fraction increases from 30% to 40%. Here, the force between the particles is not directly dependent on the applied field but on the effective field in the suspension (Lemaire and Bossis, 1991). The effective magnetic field H_{eff} is given by $H_{\text{eff}} = H - 4\pi M$. M is the magnetization and it is given by $M = \chi H_{\text{eff}}$. So $H_{\text{eff}} = H / \mu(H_{\text{eff}})$, where $\mu(H) = 1 + 4\pi\chi(H_{\text{eff}})$ is the permeability of the suspension. The permeability increases with increasing of the volume fraction and then the force between the particles decreases. However, the increasing of the volume fraction will lead the number of the chains increase and the force raise. There must be a competition between the permeability and the volume fraction. Thus the normal forces depend on both of the magnetic field and the volume fraction.

Notably, the zero applied field value of normal force is negative, which means the MR suspensions attract the plate come together. Here, the normal forces in the absence of magnetic field were carefully investigated and the normal force of rheometer was reset to zero before each measurements. The value of initial normal force for each sample is between -0.2 N and -0.1 N, which is bigger than the systematic errors. Therefore, the positive normal force can not be generated under a low magnetic field. As soon as the magnetic field reaches the critical value, the normal force changes from negative to positive (Insert of Fig. 2(b)). The critical value is definitely measured for each sample and depended on its volume fraction (e.g. 7 kA/m for 30% MRF). It is found that critical field strength is existed where a liquid experiences a phase transition to a solid phase (Tao *et al.*, 1989), which means chains are formed as the applied magnetic field exceeds the critical value. Below the critical value, the surface tension of the fluid and the gravity of particle adsorbed on the plate lead to a normal adsorbing effect. Then, the negative normal force is generated. Solely the critical magnetic field is reached, the normal pushing effects could overcome the attracting effect and then the normal force becomes positive.

When a magnetic field is externally applied, chains or columnar aggregates are formed in the MR suspensions (Lemaire *et al.*, 1992; Grasselli *et al.*, 1994; Fermigier and Gast, 1992; Zhou *et al.*, 1998; Furst and Gast, 2000). This microstructure transformation leads to the generation of the normal forces, as explained by See and Tanner (2003) and Laun *et al.* (2008). Fig. 3 shows the scheme for the for-

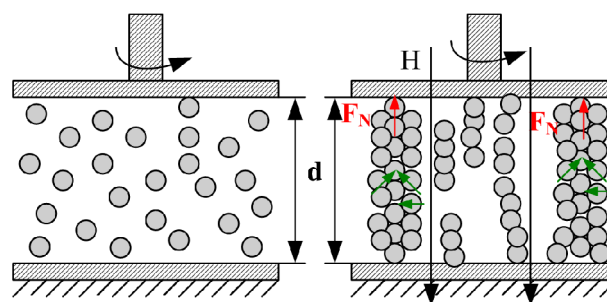


Fig. 3. (Color online) Microstructure for the origin of a positive normal force due to squeezing of magnetized spheres into existing chains.

mation of the normal force. If no magnetic field is applied, the magnetic spheres are randomly suspended in the carrier fluid and normal force could hardly be found. However, as soon as the magnetic field is applied, the iron particles in the suspensions are constrained by magnetostatic energy and then rearranged to form chains or aggregates parallel to the magnetic flux density vector, which further span plate-plate gap. The lateral forces push the spheres forward the existing chains or columns. Due to the squeezing, the existing chains or columnar aggregates are elongated along the magnetic field, which produces a force tends to push the plate apart. With increasing of the magnetic field the magnetostatic energy enhances and then the further generated normal force increases. When magnetic field strength reaches the critical value, the magnetic particles approaches their saturation magnetization, the lateral squeezing force can't be enhanced even by increasing the magnetic field. At last, the normal forces are saturated.

The gap distance d between the upper and the lower plate, which can be obtained directly from the rheometer, also changed by tuning the magnetic field. Fig. 4 shows the relationship between the average plate-plate gap and the applied magnetic field strength for 30% MR suspension measured by magneto-constant methods. The gap distance increases from 1 to 1.018 mm while the magnetic field strength enhances from 0 to 194.77 kA/m. The distance increases quickly at the beginning of the magnetic field increasing. When the magnetic field is larger than 125kA/m, the increasing velocity decreases and the gap distance tends to level off. Here, the change tendency of the gap distance is similar with the normal force because the gap variation comes from the normal force. With increasing of the applied field, the normal forces push the plate and raise the gap distance. At last, the gap distance reach plateau at large fields. It is reported (Shkel and Klingenberg, 2000) that the MR suspension often shows a typical magnetostriction property. Our work directly supports this view. Notably, the gap variation would affect the magnitude of the applied magnetic field. Here the variation is small and thus the influence of the magnitude of the applied magnetic field is

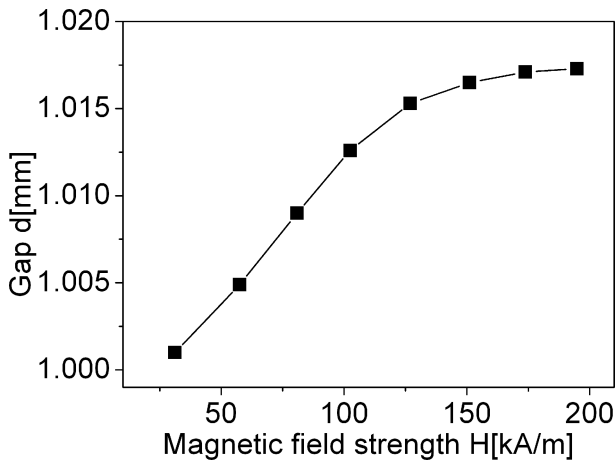


Fig. 4. Average plate-plate gap with the magnetic field strength for 30% MR suspension measured by magneto-constant method.

ignored. When the MR suspension pushes the plate, the plate would push the sample in return. There must be a compression effect on the MR suspension. The suspension works in a squeezing model (Li and Zhang, 2008) and this is the reason why normal force generates.

3.2. Power-law and magnetization model

It has been predicated by Shkel and Klingenberg (2000), without shearing and the MR fluid are treated as continua with linear, homogeneous, and anisotropic permeability properties, the normal force or normal stress with magnetic field strength can be expressed as $F_N \propto \sigma_{33} \propto kH^n$, k relates to the material magnetostriction coefficient and magnetic susceptibility and $n=2$. Here a modified magnetization model was also employed (Zubieta *et al.*, 2009) to describe the relation between normal force and magnetic field, which can be expressed by the following equation

$$F_N = F_N + (F_{N0} - F_{N\infty})(2e^{-\alpha H} - e^{-2\alpha H}) \quad (1)$$

where F_N stands for the formal force with magnetic field strength. F_N is ranged from zero applied field value F_{N0} to the saturation value $F_{N\infty}$. H is magnetic field strength and α is saturation moment index of normal force F_N . As shown in Fig. 5, both the power-law equation and magnetization model are used to fit the normal force of 30% MRF, where F_{N0} , $F_{N\infty}$, α are -1.43, 34.43, 0.013 and k, n are 0.0033, 1.89 respectively. The magnetization model can fit the curve better than the power-law equation at all the range of magnetic field strength including saturation appearances, while power-law equation can only coincide with static normal force at low magnetic field.

All other volume fraction MR suspensions were studied and the normal force was fitted by both models and the parameters are shown in Table 1. For power-law equation the exponent n is less than or equal to 2, which maybe relates to the inhomogeneity of the applied field and that

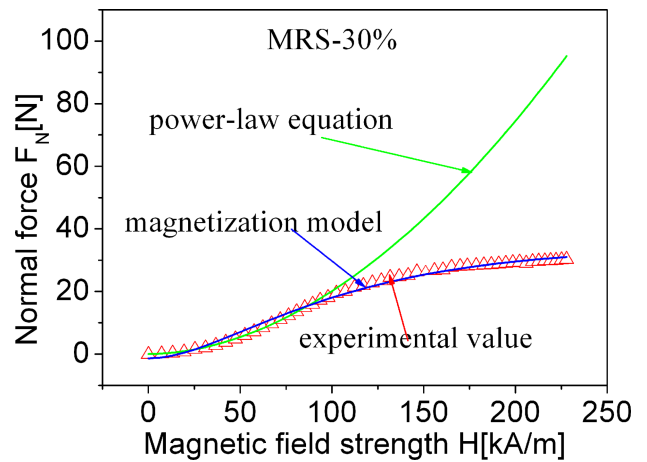


Fig. 5. (Color online) Static normal force as a function of magnetic field strength using the power-law equation and magnetization model for 30% MRF.

Table 1. Parameters of static normal force for power-law equation and magnetization model.

Model	Value	MRS			
		10%	20%	30%	40%
Power-law equation	$k[\text{N}/(\text{kA/m})^n]$	0.022	0.0059	0.0033	0.0015
	n	1.15	1.71	1.89	2
Magnetization model	F_{N0} [N]	-0.064	-0.94	-1.43	-2.47
	$F_{N\infty}$ [N]	4.96	20.44	34.34	70.41
	α [m/kA]	0.022	0.017	0.013	0.0075

the MR fluids aren't perfect transverse isotropic materials (López-López *et al.*, 2010; Andablo-Reyes *et al.*, 2011; Orellana *et al.*, 2011). The index increases with the increasing volume fraction of MRF, as the dense networks exist in high concentration samples, and the multibody effects can significantly increase the chain's microstructural strength compared to the single-width isolated chain, which mainly forms in the low concentration fluids (Fermigier and Gast, 1992; Furst and Gast, 2000). For magnetization model, the saturation normal force tested with magneto-sweep method is about 5, 20, 34, and 70N for these samples, respectively. The saturation value $F_{N\infty}$ increases with increasing of the volume fraction, due to the high fraction MFS can form more chains and aggregates as previously mentioned. The saturation index α decreases with increasing of the volume fraction which means high fraction suspensions need large saturation magnetic field strength and the index inverses to the saturation magnetic field strength.

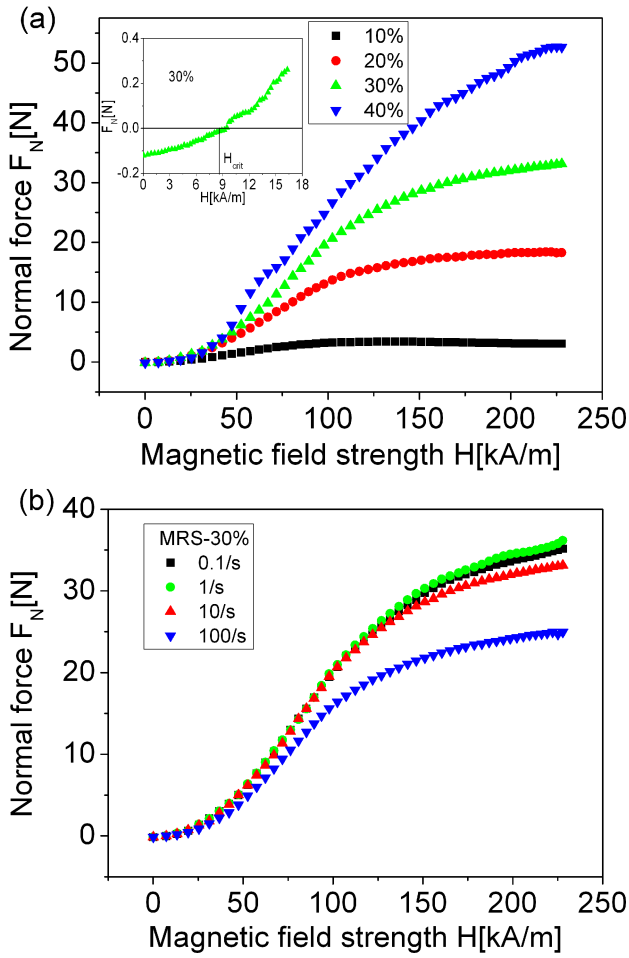


Fig. 6. (Color online) Dynamic normal force measured by magneto-sweep method with magnetic field strength for (a) all the samples at a shear rate of 10/s and (b) 30% MRS at shear rates of 0.1, 1, 10, 100/s (the insert of (a) shows the normal forces of 30% MRF at small magnetic field).

3.3. Dynamic normal force

Magnetic field dependent dynamic normal forces of 30% MR fluid were measured at a constant shear rate of 1/s (Fig. 1). When the magnetic field is applied, the dynamic normal force generates. For the constant magnetic field the most noticeable aspect is the oscillation in the dynamic normal force and the period is about 62.8 seconds. For the rheometer rotation tool, the shear rate of the rotation axis $dy/dt=R\omega/h$ is 1/s, and the rotation period T can be obtained as $T=2\pi/\omega=2\pi R/h/(dy/dt)=2\pi=62.8$ second (ω is angular speed, R is the radius of the plate and h is the gap between the plates). The rotation period of the axis is equal to the oscillatory period of the dynamic normal forces. Besides, similar oscillation normal forces could be found for other shear rates, and the periods are the same with the rotation of the rotation axis. Therefore, the oscillatory normal forces must arise from the rotation of the axis, which means that the oscillation must come from the plate mis-

alignments (Andablo-Reyes *et al.*, 2011; Orellana *et al.*, 2011). The two plates defining the gap are not precisely perpendicular to the rotation axis but tilted by a small angle. The upper plate moves with fixed angular speed while the lower plate remains stationary, the two plates rotate in and out of alignment with period the full rotation of the rotation axis. Therefore, the dynamic normal forces oscillate with the same period.

Interestingly, the dynamic normal force in every period keeps almost constant for the same magnetic field. That means a steady microscopic structure can be formed more quickly at steady flow than at rest. The dynamic normal force tested during a long time or short time is almost the same. There is no need to wait for 10 min to get a steady value such as for the static normal force. Hence, the dynamic normal forces measured with magneto-constant and magneto-sweep method are almost the same. As is similar to the static normal force characterization (Fig. 2), the dynamic normal force increases with increasing of the magnetic field and it tends to be saturated finally at high magnetic field. Besides, the negative dynamic forces exist without externally applied magnetic field (Insert of Fig. 6(a)). Dynamic normal forces at different shear rates (e.g. 0.1/s, 1/s, and 100/s) have been measured with magneto-sweep method and the same tendency can be found (Fig. 6(b)). Recently, López-López *et al.* (2010) have given an expression for the first normal stress difference and the second normal force difference for MR fluids at shearing in the considered range of magnetic fields

$$N_1 = \frac{\Phi}{\Phi_a} \mu_0 H^2 \left[-\frac{1}{4} \kappa \sin(4\theta) + \frac{1}{2} \lambda \sin^2(2\theta) \right] \quad (2)$$

$$N_2 = \frac{\Phi}{\Phi_a} \mu_0 H^2 \left[\frac{1}{2} \kappa \sin(2\theta) \cos^2 \theta - \frac{1}{4} \lambda \sin^2(2\theta) \right] \quad (3)$$

where μ_0 is the magnetic permittivity of free space, Φ is the volume fraction of magnetic particles in MR fluids, $\Phi_a \approx 0.64$ is supposed to be the internal volume fraction of the aggregates, κ and λ are dimensionless parameters and the angle θ is tilt angle of aggregated particles. So at a constant shear rate the dynamic normal forces without considering the inhomogeneity of the applied field can simplify to

$$F_N = \frac{1}{2} \pi R^2 (N_1 - N_2) \propto H^2 \quad (4)$$

where R is the radius of the plate. Therefore, a similar square relation between dynamic normal forces and applied magnetic field can be obtained in the linear permeability region. Besides, the magnetization model can also be utilized to fit the dynamic normal forces for all the region of magnetic field (not shown here for brevity).

However, the dynamic normal force doesn't increase monotonously with shear rates (Fig. 6(b)). For example, the normal force tested under a shear rate of 1/s is larger

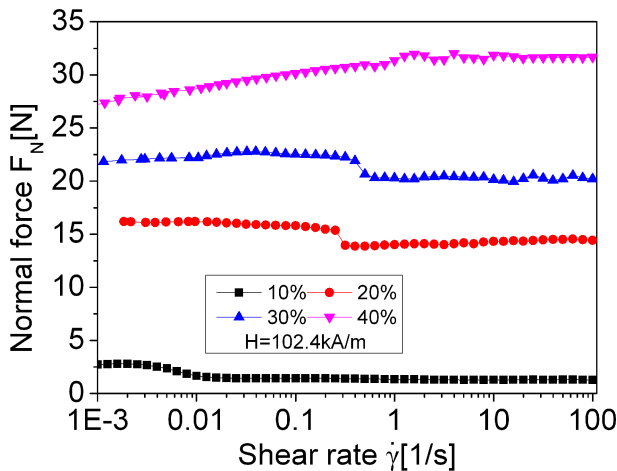


Fig. 7. (Color online) Dynamic normal forces with shear rates for all the MR fluid samples.

than the one under 0.1/s but smaller than the one under 10/s. Therefore, the dependency of dynamic normal force on the shear rates under a constant magnetic field was investigated. At a constant magnetic field of 102.4 kA/m (Fig. 7), the dynamic normal forces of four samples are obtained where the shear rate increases logarithmically from 0.001 to 100/s. Similar with López-López's results (2010), three regions can be found through the dynamic normal force vs. shear rate curve for the 10% MR fluid: (i) vertical gap-spanning structure region (shear rate is less than 0.005/s) where normal force is a plateau value; (ii) tilted gap-spanning structure region where the normal force diminishes; (iii) non-gap-spanning structure region where the normal force reaches another plateau value. Besides, the decrease of the shear stress at a low shear rate region in the case of electrorheological fluids has been observed (Choi *et al.*, 2009; Liu *et al.*, 2010). For the 20% and 30% samples, the normal forces increase considerably with increasing of the shear rate, but abruptly decrease at a shear rate of 0.3/s and then reach a steady value. This is identical with Tian's experiments (2011). At such volume fraction samples the López-López's titled gap-spanning structure region is hardly observed. For the 40% MR fluid, the normal forces increase obviously with increasing of shear rates and then tend to a steady value where shear rate is 1/s. No suddenly decreasing (normal forces) are found with the shear rates. Besides, the same could be found for other magnetic fields. So the dynamic normal force with shear rate curves dependent on the volume fractions of MR fluids. This phenomenon can be attributed to the microscopic structure transformation of MR suspensions at steady flow.

The microstructure transition has been observed by Klingenberg *et al.* (1990) for a steady flow behavior of ER suspensions and by Claracq *et al.* (2004) for the MR suspensions. When the shear rate is smaller than the critical value, the chains between the plates remain intact and start

to tilt away from electric flux direction. Therefore, similar effect will lead to the increasing of the normal forces due to shearing induced magnetic torque (Vicente *et al.*, 2002). When the shear rate reaches the critical value, for the small volume sample (*e.g.* 10%), the isolator chains or columnar adhered to the plates are mainly formed under applying the magnetic field. They would be destroyed and the effect to push the plate is weakened and thus the normal force decreased. However, with further increasing of the shear rate, the breaking of the structures by the shear and the rebuilding by the applied magnetic reach new balance and the normal forces keep steady values. For the large volume fraction MR fluids (*e.g.* 40%), not only the chains but also dense networks exist after applying the magnetic field. When the shear rate reaches the critical value, the rebuilding effect may exceed the breaking effect and the new balance structure forms and normal forces don't decrease with the shear rates. For the 20% and 30% MR fluids, when the shear rate exceeds the critical value, the new balance structure is suddenly generated but weaker than the old one, so the normal forces decrease abruptly. In addition, the larger volume fraction MRS and the higher magnetic field often lead to a higher value of critical shear rate.

3.4. Comparison of static and dynamic normal force

In this work, the differences between the static normal force and the dynamic normal force are investigated. The static normal force is measured without shearing, while dynamic normal force is measured at a shear rate of 10/s under the same conditions, as shown in Fig. 8. For 10% MRS, the static normal force is larger than dynamic normal force under all the magnetic field. However, although the static normal force of the 20% MRS is also larger than dynamic normal force at high magnetic field strength, it is found that the static normal force is smaller than dynamic normal force at low magnetic field. When the volume fraction increases to 30%, the static normal force of the MRS is almost equivalent to its dynamic force. At last, if the volume fraction of the MRS is increased to 40%, the dynamic normal force is larger than the static normal force for all the field strength. Previously, Laun *et al.* (2008) and Chan *et al.* (2009 and 2011) reported that the dynamic normal force was always larger than the static normal force. However, different results are observed in our work, which may be due to their work only focused on single volume fraction MR suspension (*e.g.* Laun *et al.*, 2008 only used 50% volume fraction MR suspension).

During the testing process, when the magnetic field was applied, the iron particles are rearranged to form chains or columnar aggregates. In this case, both complete chains adhered to the two plates and incomplete chains dispersed in fluid are formed (Fig. 3). For MR suspensions with low fraction, almost all the particles can form chains or columnar aggregates under magnetic field and a static normal

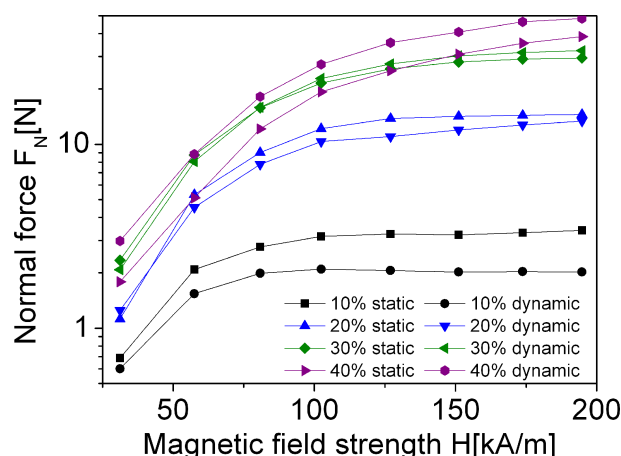


Fig. 8. (Color online) Static and dynamic normal force (shear rate is 10/s) with magnetic field strength for all the samples.

force is generated. Here, the attracting effects between chains are weak. When the shearing is applied, some chains and aggregates break and rearrange, which will weaken the pushing effect to the upper plate. Therefore, the dynamic normal force is smaller than the static normal force. For high fraction MR suspensions, more complete chains and incomplete chains are existed in the suspension in comparison to the low fraction MR suspensions. When a shearing is applied, new complete chains may be formed due to the particle rearrangement under such a dynamic shearing process. The increasing of the complete chains can enhance the pushing effect, thus the dynamic normal force is larger than static normal force. For the intermediate fraction sample, due to the poor constraint of magnetic energy under low magnetic field, more incomplete chains can be rearranged to form chains and dynamic normal force becomes larger than the static normal force. In contrast, under high magnetic field the magnetic energy constraints almost all the particles to form chains adhered to both plates. Under shearing, the chains break down and the pushing effect becomes weak, and then the dynamic normal forces decrease. As a result, the dynamic and static normal forces of the MRS are highly dependent on the volume fraction and magnetic field.

Because the dynamic normal forces change with shear rates (Fig. 6), some differences are found between the static and dynamic normal forces of different shear rates. Similarly, for 10% MR fluids, the static normal forces are always larger than the dynamic normal forces with shear rate from 0.001 to 100/s. For 40% MR fluids, the dynamic normal forces with shear rate from 0.001 to 100/s are also larger than the static normal forces. However, for the intermediate fraction sample (20% and 30%), the comparisons between the dynamic and static normal force dependent not only on magnetic field but also on the shear rates. For instance, at a certain magnetic field, the static normal force is smaller than

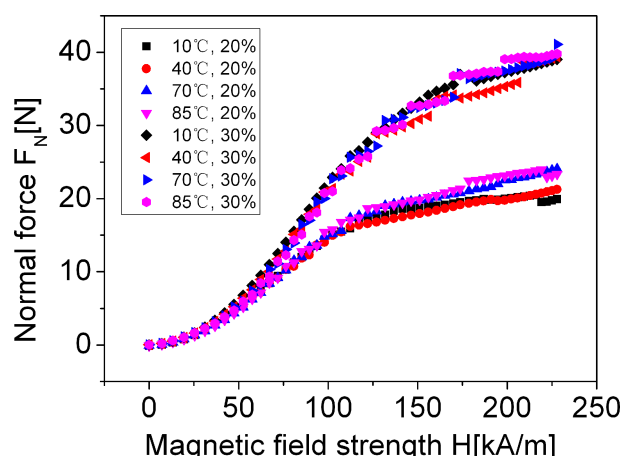


Fig. 9. (Color online) Static normal force with magnetic field strength at various temperatures for 20% and 30% MRF.

the dynamic normal force at a small shear rate but larger than the dynamic normal force at a large shear rate.

3.5. Temperature effect on static and dynamic normal force

Temperature effect on static and dynamic normal force is also investigated. Fig. 9 shows the static normal forces measured by magneto-sweep experiments at four temperatures (10°C, 40°C, 70°C, 85°C for 20% and 30% MR suspensions). It is found that at different temperatures the static normal forces vary inconspicuously under low magnetic field but increase slowly at high magnetic field strength. A similar phenomenon is observed for the dynamic normal force. As shown in Fig. 10, the dynamic normal force (at a shear rate of 10/s) increases with the increasing of temperatures for both samples under a high magnetic field. It is reported that the shear stress decreases with the increasing of temperature (Weiss and Duclos, 1994; Sahin *et al.*, 2009), which must be due to the variation of the particle volume fraction caused by expansion and contraction of the carrier oil. In this case, with the increasing of the temperature, the viscosity of the carrier oil decreases. More complete chains may be formed, which further enhance the normal response of particle to push the plate. Dynamic normal forces increase more obviously than static normal force with the increasing of temperature at high magnetic field, which indicates a stronger microstructure can be formed for dynamic normal force. Besides, for the 10% and 40% MR fluids the same temperature effect on the normal forces can be obtained (not shown here for brevity).

4. Conclusions

In this paper, a systemically experimental investigation on the normal force behavior of MR suspensions is

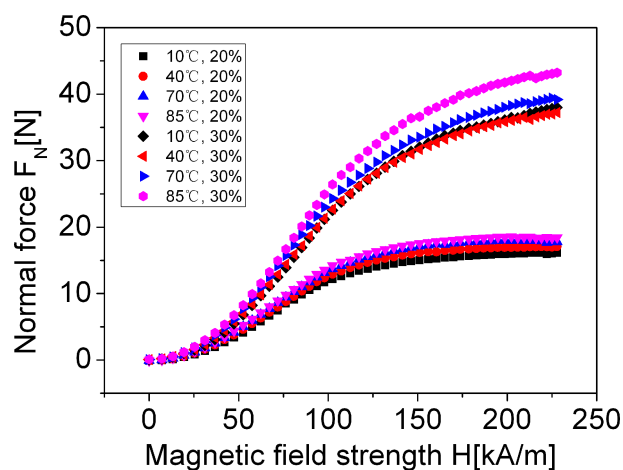


Fig. 10. (Color online) Dynamic normal force (shear rate is 10/s) with magnetic field strength at various temperatures for 20% and 30% MRF.

reported. A series of magnetorheological suspensions with different iron volume concentrations (10%, 20%, 30% and 40%) are prepared, and both the static normal forces and dynamic normal forces are measured by using a commercial plate-plate magneto-rheometer under constant and sweeping magnetic field. It is found that a critical magnetic field value is needed to generate the static and dynamic normal force. Normal forces firstly increase with the increasing of magnetic field strength, and then it reaches a saturation value. A magnetization model is proposed to describe the variation of both normal forces and the saturation static normal force calculated by this model is about 5, 20, 34, 70 N for the samples, respectively.

The dynamic normal forces at a constant shear rate have a period with the rotation of the rheometer tool, which may arise from the plate misalignments. Their changes with shear rates are different for the various samples. For the low concentration MR fluids, three regions could be easily found. For the intermediate concentration MR fluids, the dynamic normal forces suddenly decrease at the onset of the shear rate. For the high concentration fluid, the dynamic normal forces don't decrease with the shear rate.

Comparison between static normal forces and dynamic normal forces is made. The static normal force is larger than dynamic normal force for low fraction suspensions, but smaller than dynamic normal force at high volume fraction of samples. For intermediate volume fraction, they are almost equal. Therefore, the dynamic and static normal forces of the MRS are highly dependent on the volume fraction, magnetic field and shear rates.

The temperature effect on both static and dynamic normal force at low magnetic field strength could be ignored, while they increase slightly with the increasing of temperature at high magnetic field, which could be attributed to the decreasing viscosity of the carrier oil.

Acknowledgement

Financial supports from the National Natural Science Foundation of China (Grant No. 11125210), the National Basic Research Program of China (973 Program, Grant No. 2012CB937500) and the Funds of the Chinese Academy of Sciences for Key Topics in Innovation Engineering (Grant No. KJCX2-EW-L02) are gratefully acknowledged.

References

- Andablo-Reyes, E., J. de Vicente and R. Hidalgo-Alvarez, 2011, On the nonparallelism effect in thin film plate-plate Rheometry, *J. Rheol.* **55**, 981-985.
- Andablo-Reyes, E., R. Hidalgo-Alvarez and J. de Vicente, 2011, Controlling friction using magnetic nanofluids, *Soft Matter* **7**, 880.
- Carlson, J. D., D. M. Catanzarite and St K. A. Clair, 1996, Commercial magnetorheological fluid devices, *Int. J. Mod. Phys. B* **10**, 2857-2865.
- Chan, Y. T., K. P. Liu, P. L. Wong and W. A. Bullough, 2009, The response of excited magneto-rheological fluid along field direction, *Journal of Physics: Conference Series* **149**, 012041.
- Chan, Y. T., P. Wong, K. P. Liu and W. A. Bullough, 2011, Repulsive Normal Force by an Excited Magneto-Rheological Fluid Bounded by Parallel Plates in Stationary or Rotating Shear Mode, *J. Intell. Mat. Syst. Struct.* **22**, 551-560.
- Chen, J. and W. H. Liao, 2008, Design and testing of assistive knee brace with magnetorheological actuator, *Proc. of the 2008 IEEE Int. Conf. on Robotics and Biomimetics*, 512-517.
- Choi H. J. and M. S. Jhon, 2009, Electrorheology of polymers and nanocomposites, *Soft Matter* **5**, 1562-1567.
- Claracq, J., J. Sarrazin and J. P. Montfort, 2004, Viscoelastic properties of magnetorheological fluids, *Rheol. Acta* **43**, 38-49.
- De Vicente, J., F. González-Cabellero, G. Bossis and O. Volkova, 2002, Normal force study in concentrated carbonyl iron magnetorheological suspensions, *J. Rheol.* **46**, 1295-1303.
- Fang F. F., H. J. Choi and M. S. Jhon, 2009, Magnetorheology of soft magnetic carbonyl iron suspension with single-walled carbon nanotube additive and its yield stress scaling function, *Colloids Surf. A* **351**, 46-51.
- Fermigier, M. and A. P. Gast, 1992, Structure evolution in a paramagnetic latex suspension, *J. Colloid Interface Sci.* **154**, 522-539.
- Furst, E. M. and A. P. Gast, 2000, Micromechanics of magnetorheological suspensions, *Phys. Rev. E* **61**, 6732-673.
- Ginder, J. M. and L. C. Davis, 1994, Shear stresses in magnetorheological fluids: role of magnetic saturation, *Appl. Phys. Lett.* **65**, 3410-3412.
- Grasselli, Y., G. Bossis and E. Lemaire, 1994, Structure induced in suspensions by a magnetic field, *J. Phys. II France* **4**:253-263.
- Hiemenz, G. J., W. Hu and N. M. Wereley, 2008, Semi-active magnetorheological helicopter crew seat suspension for vibration isolation, *J. Aircraft* **45**, 945-953.
- Jiang, J. L., Y. Tian, D. X. Ren and Y. G. Meng, 2011, An exper-

- imental study on the normal stress of magnetorheological fluids, *Smart. Mater. Struct.* **20**, 085012.
- Jiang W. Q., Y. L. Zhang, S. H. Xuan, C. Y. Guo and X. L. Gong, 2011, Dimorphic magnetorheological fluid with improved rheological properties, *J. Magn. Magn. Mater.* **323**, 3246-3250.
- Jolly, M. R., J. D. Carlson and B. C. Munoz, 1996, A model of the behaviour of magnetorheological materials, *Smart. Mater. Struct.* **5**, 607-614.
- Klingenberg, D. J. and C. F. Zukoski, 1990, Studies on the steady shear behavior of electrorheological suspensions, *Langmuir* **6**, 15-24.
- Kordonski, W. I. and D. Golini, 2000, Fundamentals of magnetorheological fluid utilization in high precision finishing, *J. Intell. Mat. Syst. Struct.* **10**, 683-689.
- Laun, H. M., C. Gabriel and G. Schmidt, 2008, Primary and secondary normal stress differences of a magnetorheological fluid (MRF) up to magnetic flux densities of 1 T, *J. Non-Newtonian Mech.* **148**, 47-56.
- Laun, H. M., G. Schmidt, C. Gabriel and C. Kieburg, 2008, Reliable plate-plate MRF magnetorheometry based on validated radial magnetic flux density profile simulations, *Rheol. Acta* **47**, 1049-1059.
- Lemaire, E. and G. Bossis, 1991, Yield stress and wall effects in magnetic colloidal suspensions, *J. Phys D: Appl. Phys.* **24**, 1473-1477.
- Lemaire, E., Y. Grasselli and G. Bossis, 1992, Field induced structure in magneto and electro-rheological fluids, *J. Phys. II France* **2**, 359-369.
- Li, W. H., and X. Z. Zhang, 2008, The effect of friction on magnetorheological fluids, *Korea-Aust. Rheol. J.* **20**, 45-50.
- Li, W. H., B. Liu, P. B. Kosasih and X. Z. Zhang, 2007, A 2-DOF MR actuator joystick for virtual reality applications, *Sensor Actuat. A* **137**, 308-320.
- Liu Y. D., F. F. Fang and H. J. Choi, 2010, Core-shell structured semiconducting PMMA/Polyaniline snowman-like anisotropic microparticles and their electrorheology, *Langmuir* **26**, 12849-12854.
- López-López, M. T., P. Kuzhir, J. D. G. Duran and G. Bossis, 2010, Normal stresses in a shear flow of magnetorheological suspensions: viscoelastic versus maxwell stresses, *J. Rheol.* **54**, 1119-1136.
- Orellana, C. S., J. He and H. M. Jaeger, 2011, Electrorheological response of dense strontium titanyl oxalate suspensions, *Soft Matter* **7**, 8023.
- Rabinow J., 1948, The magnetic fluid Clutch, *AIEE Trans.* **67**, 1308-1313.
- Sahin H., X. Wang and F. Gordaninejad, 2009, Temperature dependence of magneto-rheological materials, *J. Intell. Mater. Sys. Struct.* **20**, 2215-2222.
- See, H. and R. Tanner, 2003, Shear rate dependence of the normal force of a magnetorheological suspension, *Rheol. Acta* **42**, 166-170.
- Shkel, Y. M. and D. J. Klingenberg, 2000, A thermodynamic approach to field-induced stresses in electro- and magneto-active composites, In: *Tao R (ed) Proc. of the 7th Int. Conf. on Electro-rheological Fluids, Magnetorheological Suspensions, Hawaii World Scientific, Singapore*, 252-259.
- Shkel, Y. M. and D. J. Klingenberg, 2001, Magnetorheology and magnetostriction of isolated chains of nonlinear magnetizable spheres, *J. Rheol.* **45**, 351-368.
- Spencer, B. F. Jr and S. Nagarajaiah, 2003, State of the art of structural control, *J. Struct. Eng.-ASCE* **129**, 845-856.
- Tao, R., J. T. Woestman and N. K. Jaggi, 1989, Electric field induced solidification, *Appl. Phys. Lett.* **55**, 1844-1846.
- Wang, X. and F. Gordaninejad, 2009, A new magnetorheological fluid-elastomer mount: phenomenological modeling and experimental study, *Smart. Mater. Struct.* **18**, 095045 .
- Weiss, K. D., and T. G. Duclos, 1994, Controllable Fluids: The temperature dependence of post-yield properties, *Int. J. Mod. Phys. B* **8**, 3015-3032.
- Yang, Y., L. Li and G. Chen, 2009, Static yield stress of ferrofluid-based magnetorheological fluids, *Rheol Acta* **48**, 457-466.
- Zhang Z., J. Q. Zhang and J. F. Jia, 2008, Characteristic analysis of magnetorheological fluid based on different carriers, *J. Cent. South Univ. T.*, **15(s1)**, 252-255.
- Zhou, L., W. J. Wen and P. Sheng, 1998, Ground States of Magnetorheological Fluids, *Phys. Rev. Lett.* **81**, 1509-1512.
- Zubieta, M., S. Eceolaza, M. J. Elejabarrieta and M. M. Bou-Ali, 2009, Magnetorheological fluids: characterization and modeling of magnetization, *Smart. Mater. Struct.* **18**, 1-6.